The active phase of Pt(110) during catalytic CO oxidation

LUND
UNIVERSITY

Hira Qazilbash

Division of Synchrotron Radiation Research
Department of Physics
Faculty of Science

Lund University

Supervisor

Johan Gustafson

In partial fulfillment of the requirements for the degree of

Master in Synchrotron Radiation Based Science
Duration: 6 months

January 2020

Acknowledgements

I would like to acknowledge my supervisor Johan Gustafson for creating this opportunity of learning. I am thankful for all the guidance and the enlightening discussions. I would thank my co-supervisor Kim Von Allmen for the technical guidance and support during the experiment. I would also like to thank all the people from the Division of Synchrotron Radiation.

Abstract

CO oxidation is an important topic in heterogeneous catalysis, due to its role in industrial processes such as pollution reduction in the auto industry, and ethanol or other fuel production. In the automotive catalytic converters CO oxidation reduces the poisonous CO to CO_2 by reacting with O_2.

Oxidation catalysts such as Pt, Pd and Rh are frequently used as catalytic converters for CO oxidation in cars. These metals are called model catalysts, and catalytic CO oxidation over these metals is one of the most widely studied reactions in the field of surface science. Despite of extensive research, the phase responsible for the catalytic activity is still under debate.

Traditionally, such studies were done under simplified conditions, in Ultra High Vacuum (UHV). However, in real industrial operations, heterogeneous catalysts are exposed to harsh environments. This thesis reports on the active phase of Pt(110) during catalytic CO oxidation, at pressures up to 510 mbar and temperatures up to 625 K. The surface structure is studied using in situ Surface X-ray diffraction, and to study the catalytic reaction, the gas phase in the vicinity of the surface is studied using Mass spectroscopy. It was found that Pt surface oxide structures are at least as active toward CO oxidation as the metallic surface.

Apart from addressing the burning question on the active phase of Pt for CO oxidation, this knowledge will help to further solve the existing problems of CO oxidation catalysts, such as oxygen poisoning. The knowledge gained can further contribute to future development of novel heterogeneous catalysts with enhanced activity, selectivity, and improved lifetime.

Contents

List of Figures

Chapter 1

Introduction

Toxic car emissions have a deteriorating impact on air quality. According to a report published by the Royal College of Physicians in 2016, around 40,000 deaths a year in the UK are attributable to exposure to air pollution. 98% of these toxic emissions, can be converted into less harmful substances by a catalytic converter.

Automotive catalytic converters use catalysts to speed up the conversion of toxic hydrocarbons, carbon monoxide, and nitrogen oxide. A catalyst lowers the energy barriers, and thus increases the rate of a certain chemical reaction. The poisonous carbon monoxide, is transformed into carbon dioxide by catalytic CO oxidation. CO oxidation is one of the main processes employed in automotive catalytic converters, and due to its relative simplicity, one of the most commonly investigated catalytic reactions.

For non-catalyzed CO oxidation the reaction between CO and O_2 is hindered by the fact that the O atoms come in pairs. In presence of a suitable metal, such as Pd, Rh or Pt the O_2 adsorbs dissociatively on the surface, the energy barrier is lowered, and the reaction rate is increased. This adsorption, however may result in the formation of an oxide layer.

The oxidation of metals is often considered as detrimental, as it causes corrosion/erosion of the materials. But the deposition of oxygen on metal surfaces, can also prove to be advantageous. Such as, the corrosion of aluminium and stainless

steels are actually hindered by the formation of a thin oxide layer, which restricts further oxidation. The most stable phase of most metals is oxidic, which means that they will oxidize if exposed to ambient temperatures and O_2 pressures. The interaction of the O_2 molecules and the metal surface is thus one of the most sought after gas-surface interaction.

Another important effect of the O_2 interacting with transition metal surfaces is its involvement in the catalytic reactions. Depending on the catalytic properties of the metal-oxide, this may lead to either an increase or a decrease of the reaction rate. Despite of extensive research during the last two decades, it is still debated if metal-oxide layers or metallic surfaces represent the catalytically most active phase for CO oxidation [14; 25] .

Such a detailed understanding of catalytic processes is one major goal of surface science. In surface science one mostly studies single crystals in UHV to achieve a clean surface. Typical operating pressures inside an automotive or industrial catalytic reactor are much higher. Over the last decades, however, there has been a strong endeavour to do surface science studies under more realistic conditions, and bridge the so called *pressure-gap* between the experimental and industrial catalysis. We continue this effort by studying catalytic reaction over the Pt single crystal at increased gas pressure up to 500 mbar.

A similar study was conducted by M. D. Ackermann et. al [1], and based on their investigation, of the role of spontaneously formed surface oxides in a catalytic process, they concluded that the Pt(110) surface oxides have a significantly higher reaction rate than the original metallic surface catalytic activation of CO oxidation. However, it was recently demonstrated by Johan Gustafson et. al [15], that if instead of following the catalytic activation of metals, the extinction is investigated, during a very slow lowering of the temperature, it is straight forward to say whether the metal is more active than the oxide.

I have therefore investigated the CO oxidation over the Pt single crystal, during catalytic extinction. A surface sensitive technique is needed, to be able to separate the surface signal from the bulk. In this work the Surface X-ray diffraction is employed to study the surface.

1.1 Overview of the Thesis

This thesis includes, in the first four chapters, a conceptual description of surfaces, effects of gas-solid surface interactions, catalysis and X-ray diffraction along with its application to surface science. The Methods and procedures' details used in developing the work are reported in Chapter 5. Finally the catalytically active phase of Pt(110), single crystal is reported and discussed, by analysing the x-ray diffraction data together with mass spectrometry during near ambient pressure CO oxidation in the last two chapters (6 and 7).

Chapter 2

Crystal Structures

Most metals are crystalline in their solid state. In this chapter we have described the basic atomic structures of crystals, and their classification. The concepts of bulk termination, and the consequential surface structures are also included. Furthermore the effects of adsorbates on the crystal structure are analyzed in the last section.

2.1 Bulk structure

A crystal is an array of atoms, arranged in a periodic lattice. The atoms residing at the lattice points form an elementary building block that is repeated periodically in all three directions. This building block delineate the basic geometry of the atoms in the crystalline structure. This is called the unit cell. One of the simplest possible crystal structures is the simple cubic structure, where the unit cell is a simple cube with one atom at each corner. If an atom is added in the centre of the cube, the structure becomes body centered cubic (bcc). Similarly by adding one atom in the centre of each face of the cube, the unit cell becomes face centered cubic (fcc). The unit cells for these three cubic lattices are shown in Figure 2.1. The metal studied in this thesis is Pt, which has a fcc lattice.

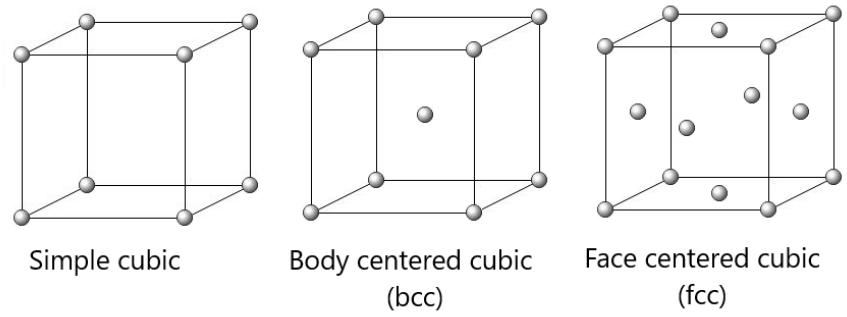

Figure 2.1: The unit cell structure.

.

2.2 Bulk terminated surface

Flat surfaces are obtained by truncating the bulk structure of a perfect single crystal. This cut can be made along any of the crystal planes. The planes are described by the Miller indices, (hkl), which are the reciprocals of the fractional intercepts which the plane makes with the crystallographic axes. A vector with the Miller indices as coordinates, is in turn perpendicular to the corresponding plane [18].

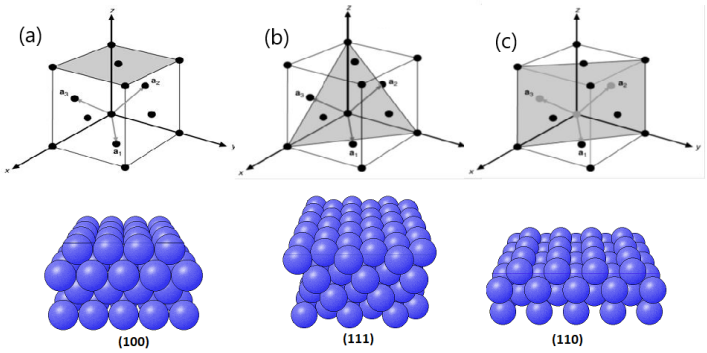

Figure 2.2: Different planes of the fcc unit cell.

.

In surface science, it is most common to study low-index surface, with only 0

and 1 as Miller indices, since these are more simple than higher-index surfaces. The three low-index surfaces of an fcc crystal are shown in Figure 2.2.

In this thesis the fcc structure used was cut along the (110) plane, shown in Figure 2.2c. The surface has a two dimensional unit cell. The surface lattice points and directions are given by the translational vectors a1 and a2. In Figure 2.3, the layer stacking in the crystal is shown. The layers underneath surface have same internal structure but they are shifted. For example in the (110) surface the structure is repeating every layer, but the in-plane position is repeating itself every second layer. Such structure is called abab stacking of layers.

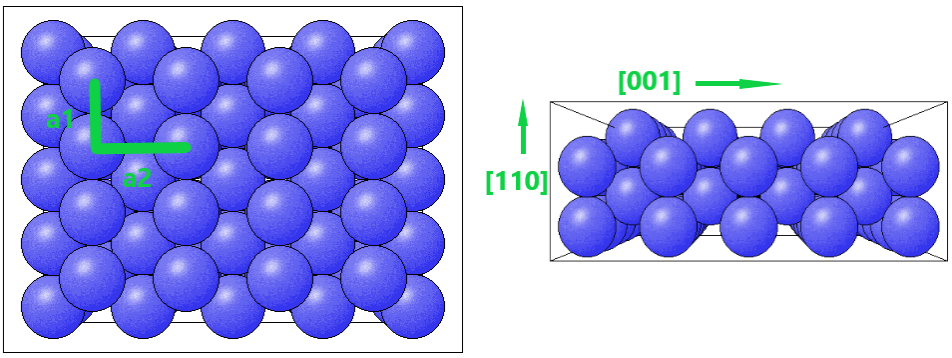

Figure 2.3: Top view and side view of fcc surface structure.

2.3 Reconstruction of the clean surface into (1x2) and Wood's notation

An ideal infinite crystal, has a non-ending periodic structure. As discussed above, this recurrent structure is terminated when the crystal is cut and a surface is created. The atoms on the surface, do not experience the same inter-atomic forces as bulk atoms. This difference causes a relaxation, and the surface atoms end up with different spacing and/or symmetry from the bulk atoms. Thus the

atomic structure of the surface can be different than the bulk. A clean Pt(110) surface is known to reconstruct to the (1×2) missing row structure, which means that the surface unit cell lengthens to twice the bulk terminated unit cell in direction perpendicular to rows, and every second row in {1-10} direction is missing as shown in Figure 2.4.

The periodicity at the surface atoms can be described using the Wood's notation:

$$(\frac{b_1}{a_1} \times \frac{b_2}{a_2})R\alpha$$

where, a_1 and a_2 are the basis vector of the bulk terminated surface lattice, while b_1 and b_2 defines the basis vectors of the surface structure unit cell. α is the rotational angle between the surface and the bulk vectors. Now the rearrangement in the surface structure can be derived from the Wood's notation. An illustration of a reconstructed structure and its representation in the Wood's notation.

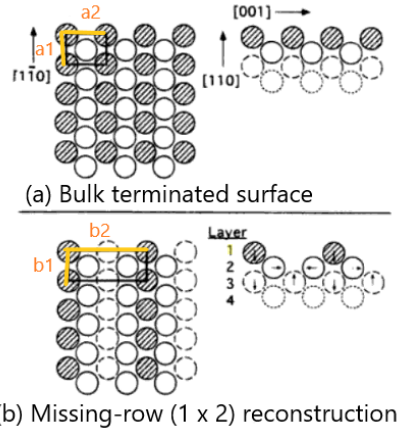

Figure 2.4: The top panel shows the unit cell vectors a_1 and a_2, of the bulk terminated surface. The bottom panel show top view of a surface with (2×1) reconstruction [6].

.

2.4 Adsorbate induces reconstructions

To study the oxides and CO induced structures, we first need to understand, the interaction of gas molecules with the surface. A molecule is said to adsorb when it interacts and binds to the surface. The adsorption may happen by chemisorption or physiosorption. Physiosorption does not include any electron transfer between the adsorbate (adsorbing gas molecule) and the substrate (adsorbing metal). The electronic structure of the atoms is essentially unchanged and the atoms form weak Van der Waals or hydrogen bonds. In contrast, chemisorption results in the formation of a chemical bond between the adsorbate and the surface. The electronic structures change and new orbitals for the valence electrons may be formed. Thus the chemisorption, affects the substrate structure. These effects can be minor such as local changes in inter-layer spacing, or major like a complete reconstruction of the surface structure [2; 18; 26]. To achieve the minimum surface free energy, the molecules adsorb at certain adsorption sites. Thus the adsorbates arrange themselves in well-ordered over-layer structures. The structure of this layer can be described using Wood's Notation in a similar manner we discussed above.

Pt(110) surface missing row reconstruction can be lifted using CO [5; 8], with adsorbate-adsorbate interaction, as the chemisorption energy of CO causes the energy balance to revert back to the (1×1) structure. The lifting of the reconstruction depends on both surface temperature and adsorbate coverage. Below 250 K the (1×2) reconstruction remains due to the immobilization of the Pt atoms [29]. In this work the (1×2) missing row reconstruction is removed by exposing the surface to 100 mbar of CO at 600 K. Just few minutes of CO exposure at this temperature, results in (1×1) bulk terminated surface, covered with CO.

2.4.1 Oxygen adsorption

A gas molecule may dissociate completely into two atoms upon adsorption. This is called dissociative chemisorption. O_2 is commonly known to adsorb dissociatively on most metals. As discussed further in Chapter 3, the dissociation of O_2 is the main barrier for CO oxidation in gas phase, and the spontaneous dissociative adsorption is the major difference to the catalysed reaction.

2.4.2 Surface Oxide

Oxygen is a highly reactive agent. Upon interaction with a metal surface, O atoms mix with the metal atoms to form metal oxide structures, if there is enough oxygen. The growth of these oxide structures can change the catalytic activity of the material.

In this work the in-plane structure of the oxide is different from bulk PtO_2 and hence called a surface oxide. Bulk oxides can be formed when the oxygen is bound to atoms beyond the surface deeper into the crystal. A previous study by Ackermann et al. showed that, during catalytic CO oxidation, two different oxide structures may form on the Pt(110) surface, as shown in Figure 2.5. To the right, is shown a one single-layer thick $PtCO_4$ carboxide, with a (1x2) periodicity, while the structure to the left is a 2-3 monolayers thick incommensurate film of PtO_2.

The Pt(110) surface oxides were reproduced in this project. The Pt surface with missing row reconstruction was first dosed with 100 mbar of CO and heated to 625 K to lift the reconstruction. The CO was then replaced with 500 mbar of O2 in order to form the oxides. As discussed further in Chapter 6.1, the results agree well with those of Ackermann, in that we were able to identify both oxide structures. However, our observations for the commensurate oxide differ significantly. They have reported a structure as essentially a carboxide, and

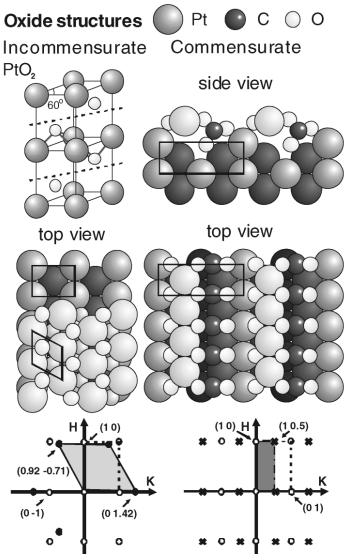

Figure 2.5: Bottom left: Pt(110) substrate structure (open circles) in reciprocal space, with the incommensurate, oxide overlayer (solid circles). Bottom right:the (1×2), commensurate oxide overlayer (crosses). All coordinates are expressed in reciprocal lattice units of Pt(110).Top and middle: Real-space structures of the oxides [1].

.

concluded that it only grows in reaction condition with partial pressures P_CO:P_O of approximately 0.2. In contrast, we grew this oxide at 500 mbar of pure O_2 flow.

Chapter 3

Catalysis

> "A catalyst is a material that accelerates a chemical reaction without affecting the position of the equilibrium and thermodynamics of the reaction."
>
> Ostwald (1895) [19].

During catalysis the reaction occur through a different path at a lower activation energy. Figure 3.1 describes the three steps of interaction between the reactants and the catalyst. The energy E_{act}, known as the activation energy, is the initial energy required for the system to break molecular bonds and form new ones. The energy difference for the reaction with and without a catalyst involved is notable.

Depending on the phase of the reactant and catalyst. Catalysis can be categorized as follows:

1. Bio-catalysis: A reaction in which, living (biological) systems, such as enzymes, are used to speed up (catalyze) chemical reaction.

2. Homogeneous catalysis: A reaction where the reactant and catalyst have same phase.

3. Heterogeneous- catalysis: A reaction in which the catalyst occupies a different phase from the reactants [24].

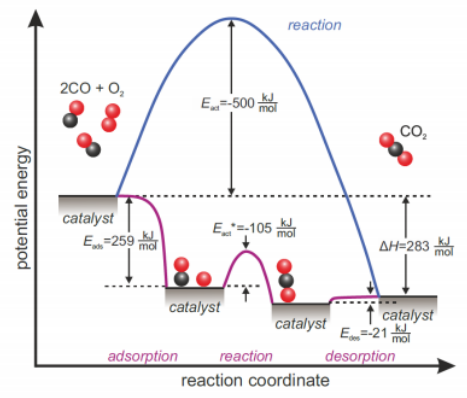

Figure 3.1: Example of energy diagram for CO oxidation on Pt(111). In blue the un-catalysed path with its activation energy, in purple the catalysed multi-step path. As can be seen the enthalpy, which defines the thermodynamic equilibrium for the reaction, is equal for both paths [12].

3.1 Heterogeneous Catalysis

In this work I have studied heterogeneous catalysis, more specifically with a solid catalyst and gaseous reactants. The reaction occurs at the interface between these phases. The catalyst provides an alternative low energy route for the reaction, by adsorbing the reactants on sites on its surface [16].

In order to gain complete knowledge of the reaction, it is important to study this interaction of gas and solid phases. The surface structure and the gas composition in the vicinity of the surface changes during catalytic reactions. Surface structures of model catalysts under highly active conditions have been studied intensively, see for instance [1; 12; 17; 21].

Catalytic converters are important material for the automobile industry. Oxidation catalyst such as platinum and palladium decreases emissions of carbon monoxide (CO) and unburned hydrocarbons (HC). As the real world catalysts

are complex material systems, and very difficult to study, single crystals, with well defined structures and characteristics are studied for the purpose of gaining a fundamental understanding of how these catalysts work. These simplified samples are called model catalysts [4; 15].

One of the most commonly investigated catalytic reaction is CO oxidation [20], and we use CO oxidation as an example for the general discussion of catalysis below. The reaction for oxidation of carbon monoxide to carbon dioxide is as follows:

$$2CO + O_2 \rightarrow 2CO_2 \tag{3.1}$$

The CO oxidation could follow three different mechanisms, established over the years to explain the reaction between two molecules over the surface of a heterogeneous catalyst [16]. These mechanisms are: Langmuir-Hinshelwood (LH), Eley-Rideal, Mars-van-Krevelen (MvK) [13]. These mechanism are further discussed below, where * denotes a vacant site.

In the **Langmuir-Hinshelwood** mechanism for CO oxidation both O_2 and CO will be adsorbed on the surface, constituting a three step reaction, Figure 3.2a. In the first two steps O_2 adsorbs dissociatively. CO then reacts with O and desorb as CO_2.

$$\begin{aligned} CO + * &\rightarrow CO* \\ O_2 + 2* &\rightarrow 2O* \\ CO* + O* &\rightarrow CO_2 + * \end{aligned} \tag{3.2}$$

In the **Eley-Rideal** mechanism, the first step is adsorption of one of the reactants on the surface. The second reactant then interacts directly with this adsorbed molecule. In the case of CO oxidation, O_2 adsorbs dissociatively and

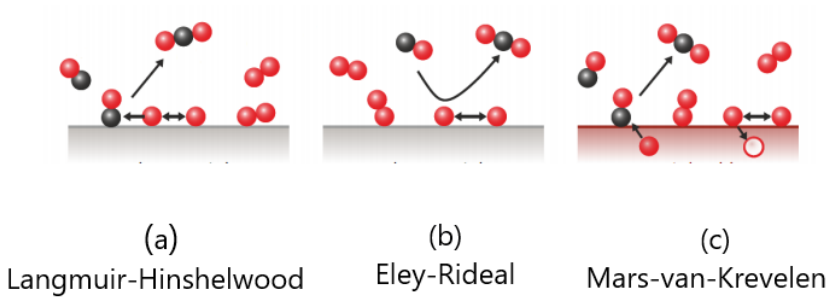

Figure 3.2: Mechanism for CO oxidation [12].

CO reacts directly with the adsorbed O,

$$\begin{aligned} O_2 + ** &\rightarrow 2O* \\ O* + CO &\rightarrow CO_2 \end{aligned} \tag{3.3}$$

For the **Mars-van-Krevelen** mechanism, the reaction starts with the adsorption of O_2 and the formation of an oxide at the surface. The second reactant then adsorbs on the oxide surface and reacts with oxygen from the oxide structure.

$$\begin{aligned} O + M + * &\rightarrow MO \\ CO + * &\rightarrow CO* \\ MO + CO* &\rightarrow CO_2 + M + * \end{aligned} \tag{3.4}$$

LH is the most generally accepted model and is how the CO oxidation reaction is believed to work at low pressures. The MvK mechanism is believed to be relevant if the oxide is the active phase, and for this to work one needs highly oxidizing conditions and the oxide needs to expose available sites for CO adsorption and reaction.

3.1.1 Heat and Mass Transfer Effects on Catalytic Activity

In this work we look at the gas composition and the surface chemistry in realistic pressures and elevated temperatures. I have studied the Pt(110) surface at increased temperature up to 650 K, in a gas mixture of O_2 and CO. In the beginning the temperature of the sample is low and the CO has the highest adsorption probability. The cold sample is thus covered with CO, obstructing O_2 dissociation at the surface. Such a surface is called CO poisoned surface as the CO prohibits the reaction. The catalytic activity is very low at this point. As the temperature increases, CO dissociates from the surface, creating vacant sites. These vacant sites can be filled by O_2, which now can dissociate and react with nearby CO and create even larger vacant surface areas. If the temperature and O_2 partial pressure is high enough, this process will go on until all the CO has been removed and replaced by O. The adsorbed O, however, does not restrict CO adsorption, and hence the reaction progresses. At this point there is a remarkable increase in the CO_2 production and the reaction rate. The catalytic activity for CO oxidation is very high. The temperature where all the CO adsorbed on the surface reacts with O_2, is called the *light off* temperature.

Since the CO oxidation is an exothermic reaction the temperature of the metal increases as a result of increase in the activity. This in return accelerates the reaction. This hike in reaction rate is critical and is known as *catalytic ignition* [9].

Beyond this activation temperature, the catalytic reaction is no longer energy or temperature dependent. It is the diffusion of the reactants to the surface that dictates the reaction rate, instead of the intrinsic activity. The reaction is now said to be mass transfer limited (MTL). At this point all of the CO reaching the surface is transformed into CO_2. Thus the gas composition near the surface

changes. The excess of O_2 in the vicinity of the surface can cause oxidation of the surface [30]. In operando experiments have shown growth of oxides simultaneous to the reaction ignition [1; 14; 25].

The reaction catalyzed by solid catalysts occurs when the reactant molecules come in contact with the active sites [17]. It is therefore imperative to study the surface structure reconstruction in correspondence to catalytic activity in order to determine these active sites.

An in-situ study at near realistic reaction conditions i.e. high pressure and temperature by Ackermann et al. suggests that the commensurate and incommensurate oxides have higher catalytic activity than the bulk terminated Pt(110) surface. They have come to this conclusion while studying the surface reconstruction of Pt(110) with a change in catalytic activity under reaction conditions. However recent studies by Gustafson et al. [15] show that a better picture of the relative activity of the metal and oxide can be seen if we follow the extinction of the catalytic reaction instead of the ignition. In this thesis we determine the active phase of the Pt(110) surface by following the catalytic extinction of the CO oxidation reaction.

As the reaction is in the MTL, after light-off and the surface is covered by an oxide, a drop in temperature lowers the reaction rate, until the MTL cannot be maintained. This will increase the CO partial pressure around the surface. Consequently, the oxide will start to reduce exposing metallic surface.

The reaction rate will increase with exposure of the metal if the metal is more active than the oxide and the reaction will be in MTL region again, with partial surface covered with oxide and the remaining is metallic. Further cooling will expose more and more metal until MTL regime is regained. If the oxide is less active, the whole surface needs to be metallic to stay in MTL, and lowering the temperature will now lead to extinction. However, if the metal is less active than

the oxide,the reaction rate should not increase with the exposure of more metal.

3.2 Transition Metal Catalyst

The elements that have a partially filled d-band, show catalytic activity. These metals are called *d-block* or transition metals. The position of the d-band compared to the Fermi levels dictates the strength of interaction between the metal and the adsorbate [10; 22].

The Platinum group metals, such as Pd, Rh and Ru have a large d-band gap from the Fermi level. This provides a sufficiently extended volume and enables partial overlap of electronic bands of metals and reactants. On the other hand open surfaces with kinks have narrow d-bands close to Fermi level. This combination makes the transition metals good catalysts, as according to the Sabatier principle the surface and adsorbate interaction should not be too weak or too strong [11]. The adsorption and desorption of the reactant gases should be balanced for the catalysis to happen.

Chapter 4

Diffraction

In this work, diffraction is used to study the surface structure, growth of oxides on the Pt surface and to monitor the alterations in the surface structure during catalysis. This chapter includes a brief description of the basic diffraction technique, and in particular surface X-ray diffraction in sections 4.1 and 4.3 respectively. Section 4.2 is dedicated to describe the concepts of reciprocal space. It is important to understand these concepts to be able to comprehend and analyse the diffraction results.

4.1 Basic Diffraction

The basic phenomenon of diffraction is scattering of light wave as it passes by a corner or through a slit. Upon interaction with a spherical object a wave is scattered in all directions. Each atom in a crystal array behaves as a scattering centre for the incoming wave. The waves scattered from two atoms in a crystal have a difference of phase related to the difference in their travelled path after scattering. As shown in figure 4.1, waves scattered by atoms separated by **R**, in two planes will have a path difference equal to d1 + d2. Assuming the scattering is elastic, a diffraction pattern occurs upon interference of these scattered waves. For constructive interference the necessary condition is that the path difference of the waves scattered from two atoms should be equal to an integer number of

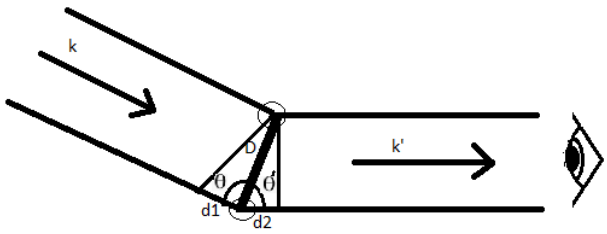

Figure 4.1: Schematic of the interference of scattered waves.

wavelengths $n\lambda$.

We can thus write the following equation.

$$\begin{aligned} path\ difference &= n\lambda \\ path\ difference &= d1 + d2 \\ &= \mathbf{R}cos\theta + \mathbf{R}cos\theta' \end{aligned} \tag{4.1}$$

The scattered wave can be described by the change in momentum. As the scattering is assumed to be elastic, i.e. $|\mathbf{k}| = |\mathbf{k'}| = 2\pi/\lambda$. The wave with addition path will have an additional phase attained by:

$$\begin{aligned} \frac{2(d1 + d2)}{\lambda} &= \mathbf{k} \cdot \mathbf{R} - \mathbf{k'} \cdot \mathbf{R} \\ \mathbf{R} &= \Delta\mathbf{k} \cdot \mathbf{R} \end{aligned} \tag{4.2}$$

for constructive interference :

$$d1 + d2 = n\lambda$$

$$\Delta\mathbf{k} \cdot \mathbf{R} = 2\pi n \tag{4.3}$$

The 3 dimensional lattice vector R is given as:

$$\mathbf{R} = m_1\mathbf{a}_1 + m_2\mathbf{a}_2 + m_3\mathbf{a}_3, \tag{4.4}$$

where a_1, a_2, a_3 are the basis vectors of the lattice and m_1, m_2, m_3 are integers. Equation 4.2 gives the condition for constructive interference in terms of wave vector.

4.2 Reciprocal Space

There are two lattices corresponding to a crystal structure. A real lattice and a reciprocal lattice. As described before the real-lattice vector $\mathbf{R}$ is given by a_j and integers m_j in equation 4.4, where as the reciprocal-lattice vector G with dimensions of reciprocal length may be expressed by b_j and integers q_j as follows.

$$\mathbf{G} = q_1\mathbf{b}_1 + q_2\mathbf{b}_2 + q_3\mathbf{b}_3, \tag{4.5}$$

We have the following relationships between the reciprocal-lattice vector $\mathbf{b}_j$ and the real-space-lattice vector $\mathbf{a}_k$.

$$\begin{gathered} \mathbf{b}_j \cdot \mathbf{a}_k = 2\pi\delta_{jk}; \\ \delta_{jk} = 0(j \neq k), \delta_{jk} = 1(j = k) \end{gathered} \tag{4.6}$$

The reciprocal lattice is the Fourier transform of the real lattice. It is a lattice in the momentum space. Thus **k**, **k'** and $\Delta\mathbf{k}$ are vectors in reciprocal space and can be expressed as:

$$\Delta\mathbf{k} = h\mathbf{b}_1 + k\mathbf{b}_2 + l\mathbf{b}_3 \tag{4.7}$$

Now combining this with equation 4.2, for the constructive interference condition, we get

$$\begin{aligned}\Delta\mathbf{k}\cdot\mathbf{R} &= 2\pi n(m_1\mathbf{a}_1 + m_2\mathbf{a}_2 + m_3\mathbf{a}_3)\cdot(h\mathbf{b}_1 + k\mathbf{b}_2 + l\mathbf{b}_3)\\ &= (m_1h + m_2k + m_3l)2\pi \\ &= 2\pi * integer\end{aligned} \tag{4.8}$$

Thus $\Delta\mathbf{k}$ is a lattice vector in reciprocal space. Now taking the product of the lattice vectors in the reciprocal G and direct R spaces we have,

$$\begin{aligned}\mathbf{R}.\mathbf{G} &= (m_1\mathbf{a}_1 + m_2\mathbf{a}_2 + m_3\mathbf{a}_3).(q_1\mathbf{b}_1 + q_2\mathbf{b}_2 + q_3\mathbf{b}_3)\\ &= (m_1q_1 + m_2q_2 + m_3q_3)2\pi \\ &= 2\pi * integer\end{aligned} \tag{4.9}$$

From equation 4.8 and 4.9, we can conclude, $\Delta\mathbf{k} = \mathbf{G}$ in order to achieve constructive interference. We will obtain constructive interference only when $\Delta\mathbf{k}$ is a reciprocal lattice vector. These constructive interference points are called Bragg points. These points scan the lattice of diffracted X-rays.

The reciprocal lattice has an inverse or reciprocal relationship to the crystal lattice. The lengths of the basis vectors in the reciprocal lattice are inverted, as shown in Figure 4.2.

4.3 Surface Xray Diffraction(SXRD)

Unlike an infinite crystal, the reciprocal lattice of a truncated crystal, that is a crystal with a surface does not contain reflections at bragg points only. The intensity is not zero between the substrate Bragg peaks, perpendicular to the surface. It is instead, smudged between these point forming rods of intensity. These rods are called Crystal Truncation Rods (CTRs). We looked at the CTR for reflection around (1 0 l) for the Pt(110) crystal. The sample and the detector were oriented such that the (0, -1.42. 0.3) point of the incommensurate oxide rod

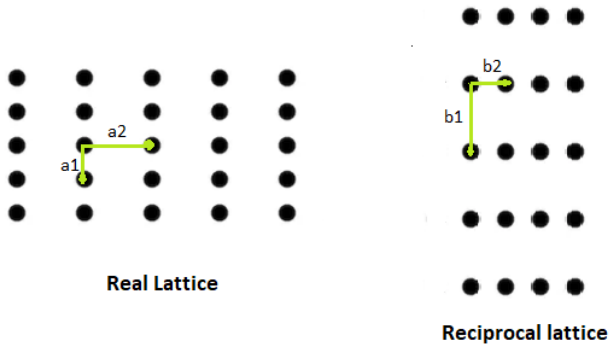

Figure 4.2: The real lattice and the reciprocal lattice.

is found in our pre-defined region of interest (ROI) in, the middle lower part of the detector. A loop scan around the (1 0 1) reflection was recorded with 80 exposures separated by 0.1deg in θ. The highest intensity, for a single exposure, at each pixel during the whole scan was calculated and assigned to the corresponding pixel.

To identify the surface structure now, only h and k integer values are required, one does not have to consider l. The condition for constructive interference, previously given by equation 4.7, now changes to:

$$\Delta\mathbf{k} = h\mathbf{b}_1 + k\mathbf{b}_2 \tag{4.10}$$

The scans along CTRs are very useful to study the vertical layers structure, which provides information on important phenomenon such as reconstruction and relaxation of surface atoms [23].

The number of atoms on the surface is very small relative to the number of atoms in the bulk of a material, A typical surface has 10^{15} atoms/cm^2 and 0.5 cm^2 of it is used in the diffraction experiment. SXRD experiments are commonly

performed at synchrotron radiation sources, however this thesis was performed using a lab source. In this work we wanted to study surface structures in presence of gas mixtures in the surface vicinity. X-rays are suitable, for such studies at high pressures as they interact weakly with matter.

A drawback with using X-ray is their large penetration depths. The scattered radiation then provides bulk structure information. To address this issue, a number of steps are taken.

1. Scan the reciprocal lattice away from the bulk reflections. For example at non-integer l values (the CTRs).

2. Approach the sample with grazing angle geometry. The surface signal is significantly increased by the grazing incidence, especially when the incidence angle is lower than the critical angle for total reflection. In this work the angle of incidence was set close to the critical angle for total reflection [$\approx 0.2^{\circ}$].

X-ray diffraction from the bulk were also measured at utilized in this experiment. The bulk CTRs provide good reference for reciprocal lattice orientation. Also in case the surface is roughened or has some impurities, it can be identified by the decrease in the intensity at the CTRs minima [7].

4.3.1 Diffraction setup and HKL mapping

In this subsection, we explain how the detector image is mapped in the reciprocal lattice units to determine the (hkl) values at each pixel. Figure 4.3 shows the diffraction setup. As in SXRD we study the surface structure, relative to the known substrate structure, so instead of the absolute $\mathbf{Q}$ or θ values , we study the reflection positions in reciprocal lattice units, which means that the Q vector is expressed in the basis vectors of the reciprocal lattice of the sample, with b_1 and

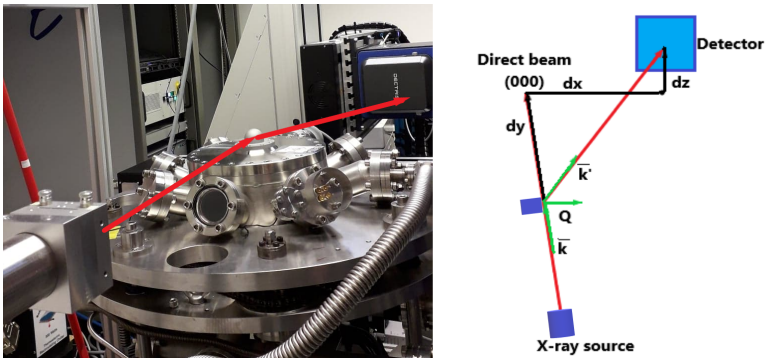

Figure 4.3: Right: Diffraction setup in lab. The red lines indicate the wave path. Left: Schematics of the diffraction setup.

b_2 being parallel to the surface and b_3 being perpendicular to the surface. The following step were taken to find the (hkl) values at each pixel on the detector:

1. We define a region of interest (ROI) at the detector around the position where the direct beam hits when the detector is in its initial position. When the detector is move, to probe other parts of reciprocal space, the direction of the scattered wave hitting the ROI is given by the vector (dx, dy, dz), where dx and dz represents how much the detector has moved in horizontal and vertical direction, respectively, while dy is the distance between the sample and the detector plane.

2. The corresponding outgoing wavevector, $\vec{\mathbf{k'}}$, is found by finding the parallel unit vector and multiplying it by the legnth of the wavevector,

$$\vec{\mathbf{k'}} = \left[\frac{[(dx, dy, dz)]}{\sqrt{dx^2 + dy^2 + dz^2}}\right] k$$

3. The scattering vector Q_{lab} is provided as the difference between k' and k,

$$\vec{\mathbf{Q}}_{lab} = \vec{\mathbf{k'}} - \vec{\mathbf{k}} = \left[\frac{[dx, dy, dz]}{\sqrt{dx^2 + dy^2 + dz^2}} - (0, 1, 0)\right] k$$

4. To set the incidence angle, the sample, and hence the coordinate system, is rotated by an angle μ around the x-axis. This is taken into account by a matrix multiplication with the rotation matrix

$$R_\mu = \begin{pmatrix} 1 & 0 & 0 \\ 0 & cos(\mu) & -sin(\mu) \\ 0 & sin(\mu) & cos(\mu) \end{pmatrix}$$

such that,

$$\vec{\mathbf{Q}}_\mu = R_\mu \vec{\mathbf{Q}}_{lab}.$$

5. Similarly, the sample may be rotated around the surface normal, which is now the z-axis, by an angle θ, defined such that the $\theta = 0$ when the incoming beam is parallel to b_2. This is taken into account by a second multiplication with a rotation matrix,

$$R_\theta = \begin{pmatrix} cos\theta & -sin\theta & 0 \\ sin\theta & cos\theta & 0 \\ 0 & 0 & 1 \end{pmatrix}$$

and

$$\vec{\mathbf{Q}}_\theta = R_\theta \vec{\mathbf{Q}}_\mu.$$

Theta (θ) is only directly given relative to the zero-position of the corresponding motor and not relative to the b_2 vector. To find it, we make use of the fact that we know which position (h,k,l) in reciprocal lattice units is probed by the ROI. Hence, we know that $\vec{\mathbf{Q}}_\theta$ is (hb_1, kb_2, lb_3). θ is the angle between the projections of $\vec{\mathbf{Q}}_\theta$ and $\vec{\mathbf{Q}}_\mu$ on the surface plane, which can be found by:

$$\theta = arccos\frac{\mathbf{Q}_\theta.\mathbf{Q}_\mu}{\mathbf{Q}^2} = arccos\frac{(hb_1, kb_2).(Q_{\mu 1}, Q_{\mu 2})}{(hb_1^2 + kb_2^2).}$$

6. The θ value is the same for all pixels on the detector. It is now straight forward to do a similar exercise for each pixel on the detector and transform the detector image to a map of the reciprocal space.

Figure 4.5 shows the detector image , mapped in (hkl), as discussed further in Chapter 4, and the commensurate oxide reflection is found at (0, -1.5, 0.28).

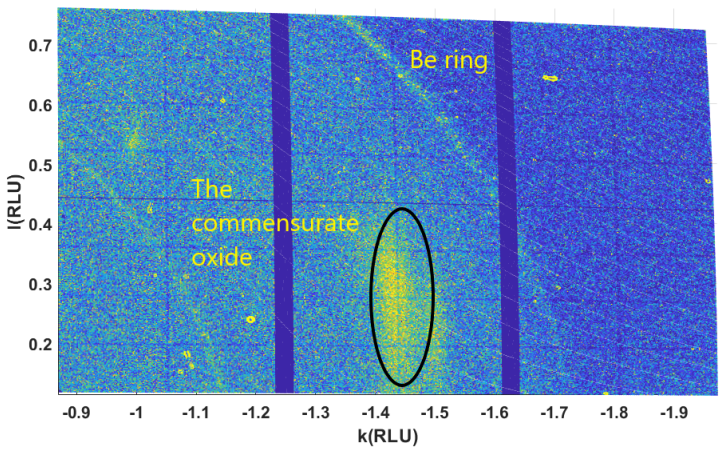

Figure 4.4: The detector imaged mapped in hkl. The position of the initial oxide structure is mapped and marked (in the black circle). This structure is calculated to be at approximately at the expected commensurate oxide position, as calculated by Ackermann [1].

Chapter 5

Experimental Methods

The in situ surface X-ray diffraction experiments were performed at the X-ray lab situated at the Astronomy building of the Lund University. The X-ray lab is a new laboratory experimental station, setup by the Division of Synchrotron Radiation Research at the Department of Physics at Lund University.

5.1 Flow Reactor Setup

The flow reactor, shown in 5.1, is a specially designed Ultra high vacuum UHV, chamber for sample preparation and reaction. The chamber has a 360° beryllium window (the Be dome is marked in Figure 5.1), for entrance and exit of the X-rays. The chamber was mounted on a z-axis goniometer with the crystal surface in a horizontal plane.
For flowing and monitoring gases through the system a custom built gas-flow system, and a mass spectrometer, used for residual gas analysis (RGA) was also employed. The gas flow system is discussed in section 5.1.1. Furthermore a complete vacuum system was used to maintain pressure.

The crystal was exposed to 16.5 KeV X-rays from a Mo kα X-ray source, with a flux of 3×10^6 photons/second, at an angle of 0.2°, and diffracted radiations were recorded at the Dectris Pilatus 300K detector.

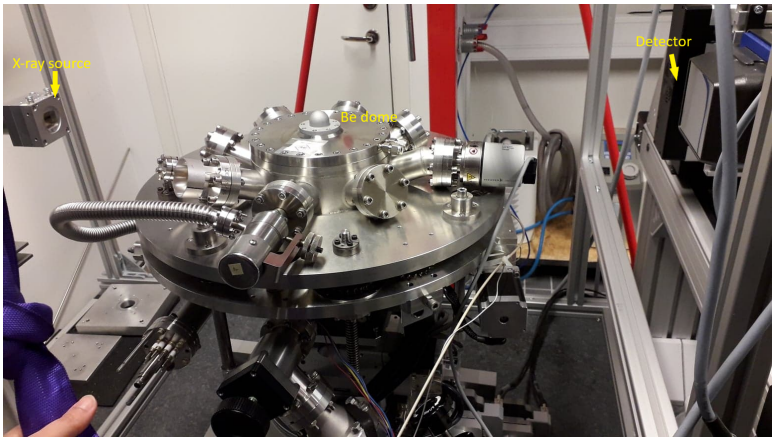

Figure 5.1: The experimental setup: Catalytic flow reactor with the source and the detector.

5.1.1 Gas-flow setup and measurements

The custom built gas-flow system with the schematics shown in Figure 5.2, was used to flow gases. The system has 5 lines in total out of which we used one for O_2, CO and Ar each. As shown in the schematics the CO line is equipped with a carbonyl trap (Gaskleen II from PALL), to avoid contamination from metal-carbonyl compounds, that otherwise may poison the sample. The gases from the bottles pass through the flow controllers, and the magnetic valves and they are mixed before going to the flow-reactor.

The output gasses are analysed by a Quadrupole Mass Spectrometer (QMS) coupled with Secondary Electron Multiplier (QMS-SEM). The QMS consists of a HiCUBE pumping station, a PrismaPlus QMG220 mass-spectrometer, both from PFEIFFER, and a cold-cathode pressure gauge for pressure regulation.

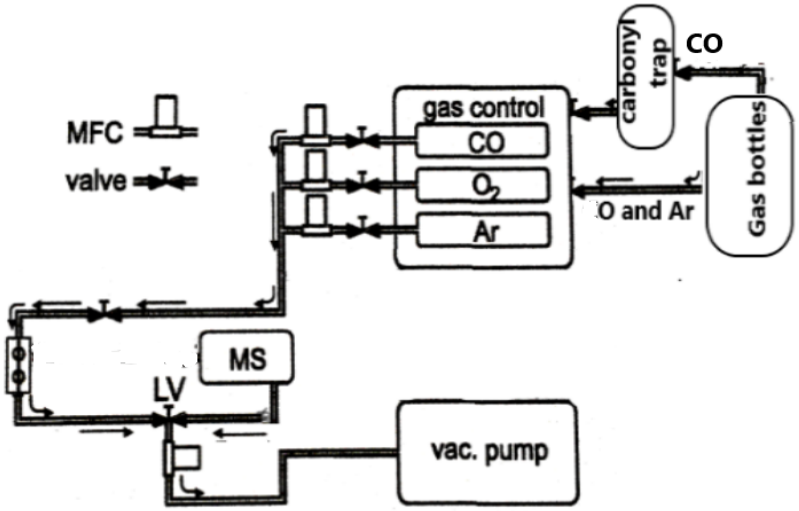

Figure 5.2: A schematics of the complete gas-mixing system: well visible the mass-flow-controllers (MFC), the cell, leak-valve (LV).

5.2 The Experiment

The Pt(110) crystal surface was sputter-cleaned by 2-keV Ar ion bombardment at 2×10^{-4} mbar pressure and 10 mA for 20 minutes, followed by annealing at $\approx$ 1100 K for 5 minutes. This cycle was repeated 3 times. The Pt (110) crystal lattice is described with a tetragonal unit cell, with $A_1 = A_3 = a_o = 2.774$ and $A_2 = \sqrt{2}a_o$. A_1 and A_2 are the perpendicular unit vectors in the surface plane, while A_3 is perpendicular to the surface, along [110].H and K are the vectors in surface plane in the reciprocal space, while L is normal to the surface.

In order to replicate the experiment by Ackermann et al., the (1×2) missing row reconstruction formed by annealing in vacuum, was first removed by exposure to CO at 600 K. Once the surface was rearranged to a (1×1) bulk terminated structure, the incommensurate oxide was formed by exposure to 500 mbar O_2 at 670 K. The Pt surface is found to be extremely difficult to oxidize and despite the

high pressure of O_2 at elevated temperature took a long time to form the stable incommensurate oxide. The incommensurate oxide at (0 1.42 0.3) in reciprocal space was achieved by flowing 500 mbar of O_2 and heating sample to 673 K. The process was followed by SXRD as reported in Chapter 6.

Once the oxide was formed, the catalytic CO oxidation reaction was started by flowing a mixture of CO:O at 1:50, with a total flow of 51 ml_n/min*[1] and a total pressure of 500 mbar. In order to study the surface alterations and catalytic activity, the sample temperature was lowered in steps, while the production of CO_2 monitored simultaneously with MS and SXRD, respectively.

In this experiment the temperature was dropped and CO_2 production rate and surface oxide presence was monitored. The extinction will illustrate the catalytically active phase, as discussed in Chapter 3. The MS data (recording CO_2 rate), and the SXRD data for oxide presence is presented in the result section.

[1] *1 ml_n=1ml at normal temperature and pressure.

Chapter 6

Results and discussion

To study the active phase during CO oxidation over Pt(110), the bulk terminated Pt surface was first oxidized under O_2 rich conditions. The results for the surface oxidation are presented and discussed in section 6.1. The detector images were mapped in reciprocal lattice units (hkl), to define each pixel position. This enabled us to identify all the reflections appearing on the detector, showing that the oxidation process went from the metallic surface via a thin commensurate oxide to a 2-3 layer thick incommensurate PtO_2 film. After introducing CO at increased temperature, the surface was found in a catalytically highly active state and the CO oxidation reaction was mass transfer limited, while the oxide structure remained at the surface. In order to compare the activity of the oxide and the metallic surface, the sample temperature was reduced and the catalytic activity and the presence of the oxide were monitored. These results are discussed in section 6.2.

6.1 Pt(110) oxidation

In agreement with the previous studies [27] we initially had a metallic, CO-saturated Pt surface, after removal of the missing row reconstruction. If O_2 is introduced at low temperatures, it is not able to dissociate as the surface is covered by CO, which poisons the reaction. As the temperature increases the

CO desorbs and the catalyst becomes active. At the light-off temperature the reaction rate increases drastically. The light-off or activation temperature in our measurements was higher than reported by Ackermann. This difference in temperature could be due to either the temperature underestimation in our setup or the fact that we performed the experiment in a flow catalytic reactor. The gas concentration gradient can differ considerably between flow and batch catalytic reactors. Furthermore, the partial pressure concentrations were also not the same as Ackermann.

In order to enable as direct comparison as possible, the preparation for the CO oxidation experiment was copied from the study by Ackermann [1]. Hence, we started by lifting the MR reconstruction by exposure to CO at 625 K before exchanging the CO with O_2 in order to form the incommensurate oxide. We then followed the oxidation process with SXRD. The starting point was a CO covered, unreconstructed surface, and the oxidation started with the replacement of the CO with O_2. The sample and the detector were oriented such that the (0, -1.42. 0.3) point of the incommensurate oxide rod is found our pre-defined region of interest (ROI) in the middle lower part of the detector. With this orientation, we can also follow the substrate CTR at (0, -1, 0.53). In addition, another rod at (0, -1.5, 0.2), which we identify as the commensurate oxide, as discussed in Chapter 4, was observed, before the appearance of the incommensurate oxide rod.

The oxidation process is followed in Figure 6.1, where the intensities (Average number of counts per pixel), for the substrate CTR and the two oxide structures are plotted as a function of time. As the oxidation process proceeds, the commensurate oxide is gradually replaced by the incommensurate one, and the inter-phase to the metal becomes rough until the CTR is not visible above the background noise after about 130 minutes, a bit before the commensurate oxide signal is gone.

The SXRD data was recorded with continuous 15 minutes exposures, to track the surface evolution in O_2 environment.

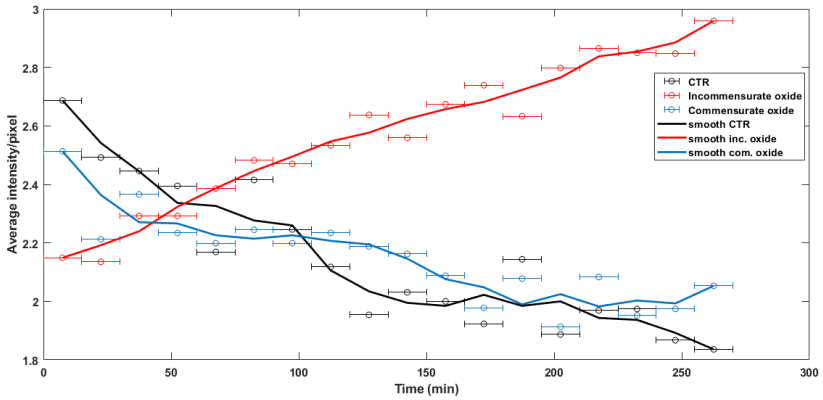

Figure 6.1: The intensities of the incommensurate oxide reflection at (0, 1.42, 0.3), the commensurate oxide at (0, 1.52, 0.2) and the CTR over time , in 500 mbar of O_2.

The unexpected part of these results is that we actually see the commensurate oxide. According to Ackermann, the commensurate oxide is a carboxide, but under these conditions, any CO left on the surface would be removed very quickly. Hence, this (and likely the oxide in Ackermann's paper) is actually not a carboxide. The actual structure of the oxide however remain to be investigated further before we can conclude anything more.

6.2 CO oxidation

The CO oxidation was studied on oxidized bulk terminated metal surface. Figure 6.2(bottom) shows operando SXRD measurements. The intensities of the incommensurate surface oxide signal around (0, -1.42, 0.3) CTR and around (0, -1) and presented as interval bars, for each exposure, that is each temperature decrement step. The intensities of the two regions of interests, ROI0: CTR reflection and ROI1: reflection from the incommensurate surface PtOx were averaged out and

plotted over time of extinction. As the oxide reduced the CTR reflection grow stronger again, indicating the reappearance of the metal surface. The experiments were performed in a flow of 50 and 1 ml_n/min*[1], of O_2 and CO, respectively, and a total pressure of 510 mbar.

The Figure 6.2(top) also contain the MS signal recorded during the deactivation of the CO oxidation reaction on the Pt(110) surface following a slow cooling process. As marked in the legend of the Figure 6.2 the blue lines represent the CO_2 RGA signal, monitoring the catalytic activity.

As the sample temperature was lowered, the reactivity did not decrease initially (CO_2 rate is almost constant in the beginning in Figure 6.2(top)), implying that the reaction is still MTL. The SXRD signal for Pt surface oxide disappears completely in conjunction with the extinction. The slight decrease in the intensity of the oxide reflections at (0, -1.42, 0.3), before the extinction, can be attributed to the roughening of the oxide layer, due to the MvK mechanism as discussed in Ref [3].

In agreement with the previous studies by Ackermann et al.[1] and in Ref. [3], our measurements also show that for CO oxidation over Pt(110), ***the Pt surface oxides are at least as active as the metal.*** They had observed the same surface oxides, and concluded that "the surface oxides found here on Pt(110) have a significantly higher reaction rate than the original metallic surface"[1].

This claim by Ackermann et al.[1] that the oxide has a high reactivity can be misleading if the drop in the initial temperature is too high and the reaction rate is not high enough to maintain MTL region. Also the CO partial pressure P_{CO} can be very low for the metal to maintain high reactivity. Ackermann et al. performed their measurements at 80 mbar CO and 500 mbar of O_2, while our data was recorded at 10 mbar CO and 500 mbar of O_2.

[1]*1 ml_n=1ml at normal temperature and pressure.

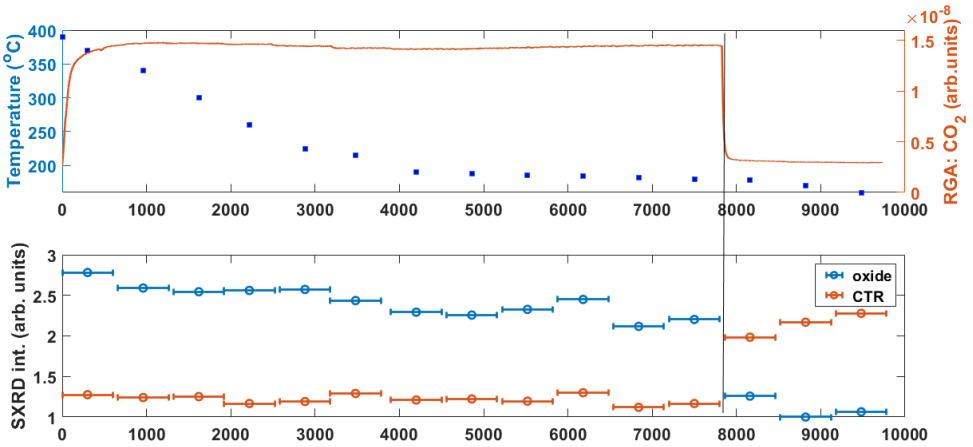

Figure 6.2: (Top):The extinction is followed while slowly decreasing the sample temperature. Mass spectrometry data (red line) and sample temperature (blue dots) showing that in the beginning of the experiments, the CO_2 production is mass transfer limited and does not depend significantly on temperature. (Bottom): Measurements for incommensurate PtO_x catalytic extinction at (0 1.42 0.3). SXRD signals from the surface oxide α-PtO_x (red bars), stays close to unaffected until extinction. SXRD signals from the surface oxide α-PtO_x (blue bars). The metallic CTR is visible as the oxide is reduced and the metallic surface is uncovered,

The high activity of Pt(110) to CO oxidation can be explained by looking at the Density Functional Theory (DFT) calculations for CO oxidation mechanisms by Qing et al. [28]. The CO oxidation mechanism is CO + O_2, which occurs at the metal/oxide with a reaction barrier as low as 0.1 eV. This molecular mechanism is favoured by the presence of O_2 molecules with high chemisorption energy [28; 31]. On one hand the reasonably high chemisorption energy may increase the coverage of O_2 on the surface increasing reaction possibility of O_2 with CO. Second, it can activate the O_2 molecule and reduce the reaction barrier. The PtO_x is not very well ordered, but grows in small domains. In the domain boundaries, there are probably a large concentration of defect sites where the CO molecules can adsorb. With such a small reaction barrier the CO molecules can react with nearby O from CO_2.

Finally, another incommensurate oxide site was studied. The sample was rotated to measure the surface oxide at (0.92, -0.7, 0.3). Similar trends for the CO_2 MS signal and the surface oxide SXRD signal were obtained. These are presented in Figure 6.3.

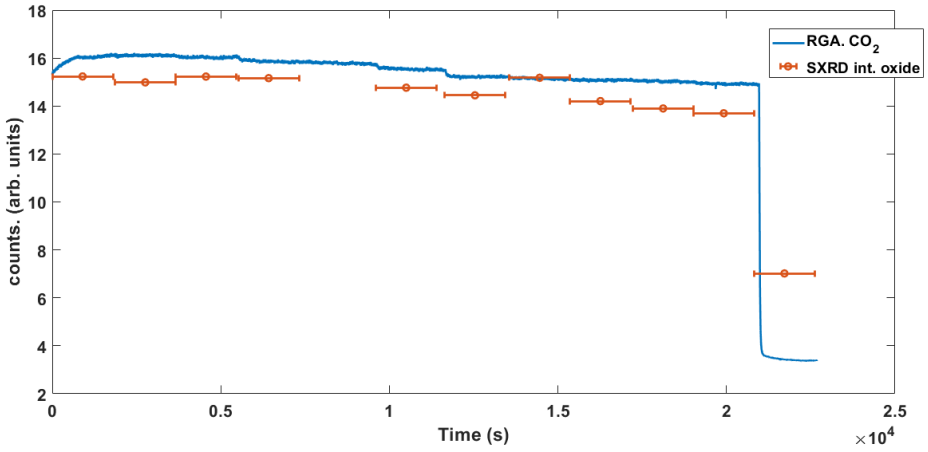

Figure 6.3: Catalytic extinction of the incommensurate oxide on Pt(110) at (0.92, -0.7, 0.3)

Chapter 7

Conclusions and outlook

To conclude, in this work the active phase for catalytic CO oxidation over Pt oxides have been studied, under relevant pressure and temperature conditions. Pt surface oxide structures were studied and catalytic activity was assessed in a lab setup using a flow reactor. The CO oxidation process proposed by Mars-van-Krevelen (MvK) is confirmed. The results show that the Pt surface oxide structures are at least as active toward CO oxidation as the metallic surface.

The active phase of Pt(110) has previously been examined during catalytic activation. In this work the catalytic extinction is studied to find the active phase. This provides a better view for the activity of the surface oxide.

We have discussed that the molecular mechanism for CO_2 production is favored on PtO_2(110). As the experiments were performed in O_2 rich environments, and the chemisorption energy is relatively high, we get large O_2 coverage on the surface, and consequently more interaction with CO. The incommensurate oxide has been studied in detail, near realistic reaction conditions, however it would be interesting to monitor the behaviour of this oxide in a batch reactor and different partial pressures of CO:O_2. I was not able to stabilize the commensurate oxide long enough to study the CO oxidation over it. From Ackermann's study, we know that the commensurate oxide needs higher CO partial pressure. The next

step could be to perform the experiment in a batch catalytic reactor, and perform the CO oxidation at 80 mbar of CO and 500 mbar of O_2. As we have observed this oxide structure does not stabilize and the surface is covered with the incommensurate oxide in a very short time, one could try to stop the O_2 flow and let the sample cool in UHV to see if this oxide structure stabilizes. The catalytic extinction can then be performed by again heating the sample and introducing CO and O over the oxidized metal.

The transition metals based catalytic converters are the most effective automotive catalytic converters. This works addresses the burning question of the active phase of Pt for CO oxidation. This knowledge will help to further solve the existing problems of CO oxidation catalysts, such as oxygen poisoning. This project is one of the first successful experiments done with the Surface diffraction setup, at the Synchrotron Radiation Division X-ray lab, where the surface structure reconstruction was observed for the first time with current setup.

The main limitations of this setup are the low intensity, and a large foot print, as compared to sample dimensions of the X-ray beam. The current source has an intensity of 6×10^6 photons/s, with a footprint of 140 mm, where as the sample is 9 mm. The new source design in planning promises a significantly smaller footprint of 23 mm with an intensity of 5×10^9 photons/s, which mean the sample will receive approximately 10^4 times higher intensity.

Higher X-ray intensity will allows measurements to be performed at a greater separation between the sample and the detector, and much faster measurement times.

References

[1] M. D. Ackermann, T. M. Pedersen, B. L. M. Hendriksen, O. Robach, S. C. Bobaru, I. Popa, C. Quiros, H. Kim, B. Hammer, S. Ferrer, and J.W. M. Frenken. Structure and reactivity of surface oxides on pt(110) during catalytic co oxidation; prl 95, 255505. 2005.

[2] A. W. Adamson. Physical chemistry of surfaces, 5th ed. (john wiley & sons, new york). 1990.

[3] B. L. M. Hendriksen and J. W. M. Frenken. Co oxidation on pt(110): Scanning tunneling microscopy inside a high-pressure flow reactor,phy. rev. lett. 89, 4. 2002.

[4] Boudart, M. Model catalysts: reductionism for understanding. topics in catalysis 13. page 147, 2000.

[5] C. M. Comrie and R. M. Lambert. Chemisorption and surface structural chemistry of carbon monoxide on pt(110),. chem. soc., faraday trans. 1, 72. pages 1659–1669, 1976,.

[6] D.A. King and D.P. Woodruff. Phase transitions and adsorbate restructuring at metal surface, v 7. 7 1994.

[7] R. Feidenhans'l. Surface structure determination by x-ray diffraction; surface science reports 10. pages 105–188, 1989.

[8] P. Fery, W. Moritz, and D. Wolf. Structure determination of the (12) and (13) reconstructions of pt(110) by low-energy electron diffraction phys. rev. b 38. page 7275, 15 October 1988,.

[9] Frank-Kamenetskii. D. a. diffusion and heat exchange in chemical kinetics; princeton university press: Princeton, nj. 2015.

[10] Freund, Hans-Joachim, Gerard, Meijer, Matthias, Scheffler, Robert Schlogl, and Wolf. Martin. Co oxidation as a prototypical reaction for heterogeneous processes. angewandte chemie international edition, 50(43):. page 10064–10094, 2011.

[11] B. Hammer and J. K. Norskov;. Why gold is the noblest of all the metals;nature volume 376. page 238–240, 1995.

[12] Uta Hejral. Operando characterization of supported alloy nanoparticles during catalytic co oxidation by surface sensitive x-ray diffraction, hamburg. 2015.

[13] Chorkendorff I. and Niemantsverdriet J.W. Concept of modern catalysis and kinetics. wiley,. 2003.

[14] J. Gustafson et al. A high pressure x-ray photoelectron spectroscopy study of co oxidation over rh(100), phys. condens. matter 26, 055003. 2014.

[15] J. Gustafson et al. The role of oxides in catalytic co oxidation over rhodium and palladium;acs catalysis. pages 8 (5), 4438–4445., 2018.

[16] Ross Julian and H.Burlington. Heterogeneous catalysis:fundamentals and applications, elsevier science. 2011.

[17] Raweewan Klaewkla, Matthias Arend, and Wolfgang F. Hoelderich. A review of mass transfer controlling the reaction rate in heterogeneous catalytic systems: Achen.

[18] Kurt W. Kolasinski. Surface science: Foundations of catalysis and nanoscience. wiley. 2012.

[19] P.W. Van Leeuwen. Homogeneous catalysis: Understanding the art springer science and business media. 2006.

[20] Edwin Lundgren and H. Over. In situ gas-surface interactions: Approaching

realistic conditions. j. phys.: Condense.matter 20. 180302. 2008.

[21] M.Shipilin et al. Quantitative surface structure determination using in situ high-energy sxrd: Surface oxide formation on pd(100) during catalytic co oxidation,surface science, volume 630. pages 229–235, 12 2014.

[22] Johan Nilsson, Per-Anders Carlsson, Fouladvand Sheedeh, Natalia M.Martin, Johan Gustafson, Mark A. Newton, Edvin Lundgren, Henrik Gronbeck, and Magnus Skoglundh. Chemistry of supported palladium nanoparticles during methane oxidation. acs catalysis, 5(4):,. page 2481–2489, 2015.

[23] I K Robinson and D J Tweet ;. Surface x-ray diffraction;rep. prog. phys.,55. pages 599–647, 1992,.

[24] Gadi Rothenberg. Catalysis: Concepts and green applications. wiley. 2010.

[25] U. Hejral et al. Identification of a catalytically highly active surface phase for co oxidation over ptrh nanoparticles under operando reaction conditions,phys. rev. lett. 120, 126101 . 03 2018.

[26] U.Starke, M.A.Van Hove, and G.A.Somorjai. Adsorbate-induced relaxations of close-packed fcc and hcp metal surfaces, progress in surface science volume 46, issues 2–3. pages 305–319, June–July 1994.

[27] "Van Spronsen, Matthijs A. and Frenken, Joost W. M. and Groot, Irene M. N. Surface science under reaction conditions: Co oxidation on pt and pd model catalysts,chem. soc. rev.,14. pages 4347–4374, 2017.

[28] Xue-Qing Gong and, R. Raval, and P. Hu. General insight into co oxidation: A density functional theory study of the reaction mechanism on platinum oxides, phys. rev. lett. 93, 106104. 9 2004.

[29] Shuichi Yamagishi, Toshiyuki Fujimoto, Yasuji Inada, and Hideo Orita. Studies of co adsorption on pt(100), pt(410), and pt(110) surfaces using density functional theory,j. phys. chem. b , 109,. pages 8899–8908, 2005,.

[30] Zetterberg et al. Spatially and temporally resolved gas distributions around heterogeneous catalystsusing infrared planar laser-induced fluorescence. nat. commun.6,. pages 70–76, 2015.

[31] Zhi-Pan Liu, Xue-Qing Gong, Jorge Kohanoff, Cristián Sanchez, and P. Hu. Catalytic role of metal oxides in gold-based catalysts: A first principles study of co oxidation on tio_2 supported au.,phys. rev. lett. 91, 266102. 12 2003.